

SUPPLEMENTARY INFORMATION

Size-resolved characterization of organic aerosol in the North China

Plain: new insights from high resolution spectral analysis

Weiqi Xu¹, Chun Chen^{1,2}, Yanmei Qiu^{1,2}, Conghui Xie^{1,2,a}, Yunle Chen³, Nan Ma⁴, Wanyun Xu⁵, Pingqing Fu^{2,6}, Zifa Wang^{1,2}, Xiaole Pan¹, Jiang Zhu^{1,2}, Nga Lee Ng^{3,7,8}, and Yele Sun^{1,2,9*}

¹State Key Laboratory of Atmospheric Boundary Layer Physics and Atmospheric Chemistry, Institute of Atmospheric Physics, Chinese Academy of Sciences, Beijing 100029, China

²College of Earth and Planetary Sciences, University of Chinese Academy of Sciences, Beijing 100049, China

³School of Earth and Atmospheric Sciences, Georgia Institute of Technology, Atlanta, Georgia 30332, United States

⁴Institute for Environmental and Climate Research, Jinan University, Guangzhou 511443, China

⁵State Key Laboratory of Severe Weather & Key Laboratory for Atmospheric Chemistry, Institute of Atmospheric Composition, Chinese Academy of Meteorological Sciences, Beijing, 100081, China

⁶Institute of Surface-Earth System Science, Tianjin University, Tianjin 300072, China

⁷School of Chemical and Biomolecular Engineering, Georgia Institute of Technology, Atlanta, GA 30332, USA

⁸School of Civil and Environmental Engineering, Georgia Institute of Technology, Atlanta, GA 30332, USA

⁹Center for Excellence in Regional Atmospheric Environment, Institute of Urban Environment, Chinese Academy of Sciences, Xiamen 361021, China

^anow at: State Key Joint Laboratory of Environmental Simulation and Pollution Control, College of Environmental Sciences and Engineering, Peking University, Beijing 100871, China

Correspondence: Yele Sun (sunyele@mail.iap.ac.cn)

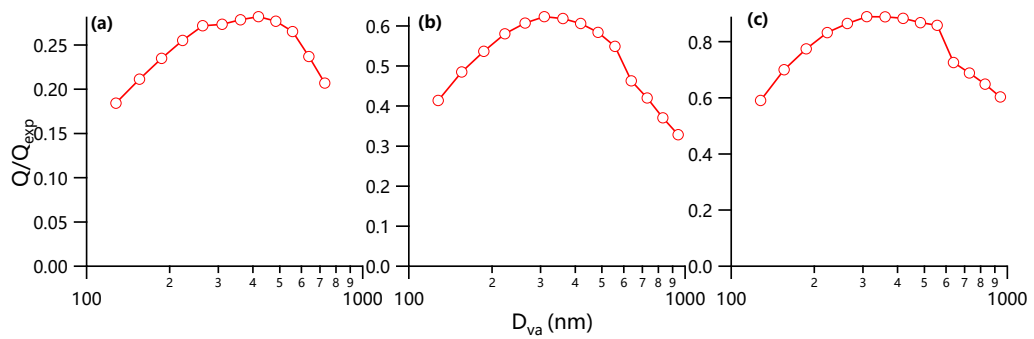


Figure S1. Size distributions of Q/Q_{exp} in (a) summer and (b) winter in Beijing, and (c) winter in Gucheng.

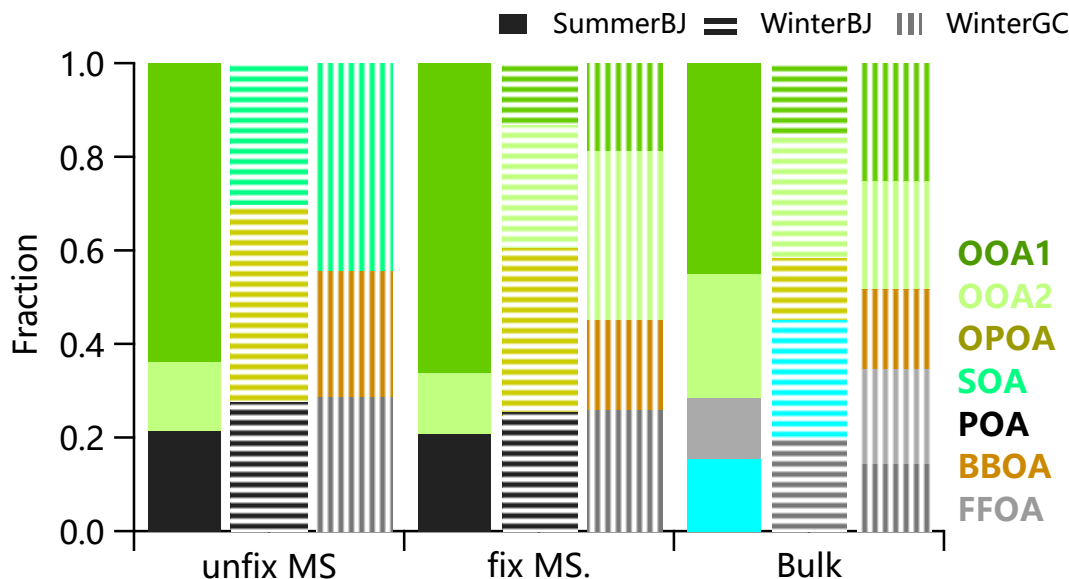


Figure S2. Average OA composition resolved by size-resolved PMF (labeled as “unfix MS”), size-all PMF (labeled as “fix MS.”), and bulk OA PMF (labeled as “Bulk”).

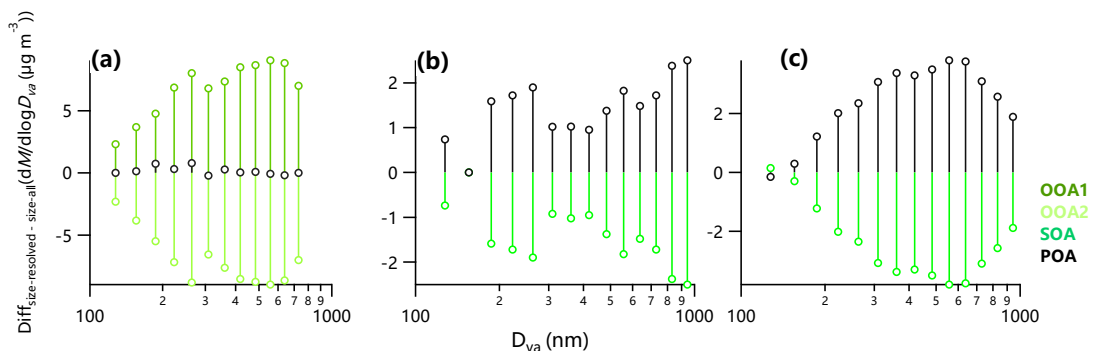


Figure S3. Size distributions of differences in mass loadings identified by size-resolved PMF and

size-all PMF in (a) summer and (b) winter in Beijing, and (c) winter in Gucheng.

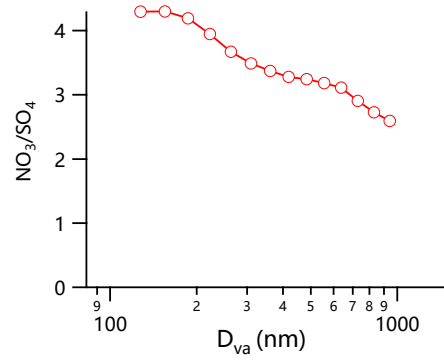


Figure S4. Size distributions of ratios of NO_3 to SO_4 in Beijing in winter.

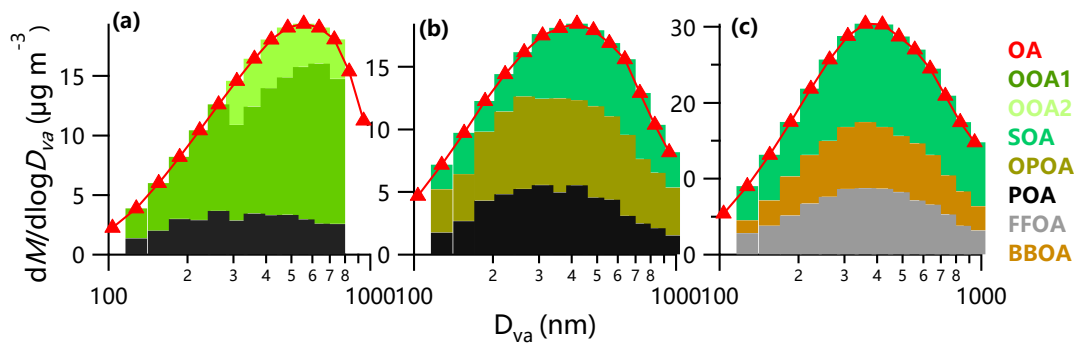
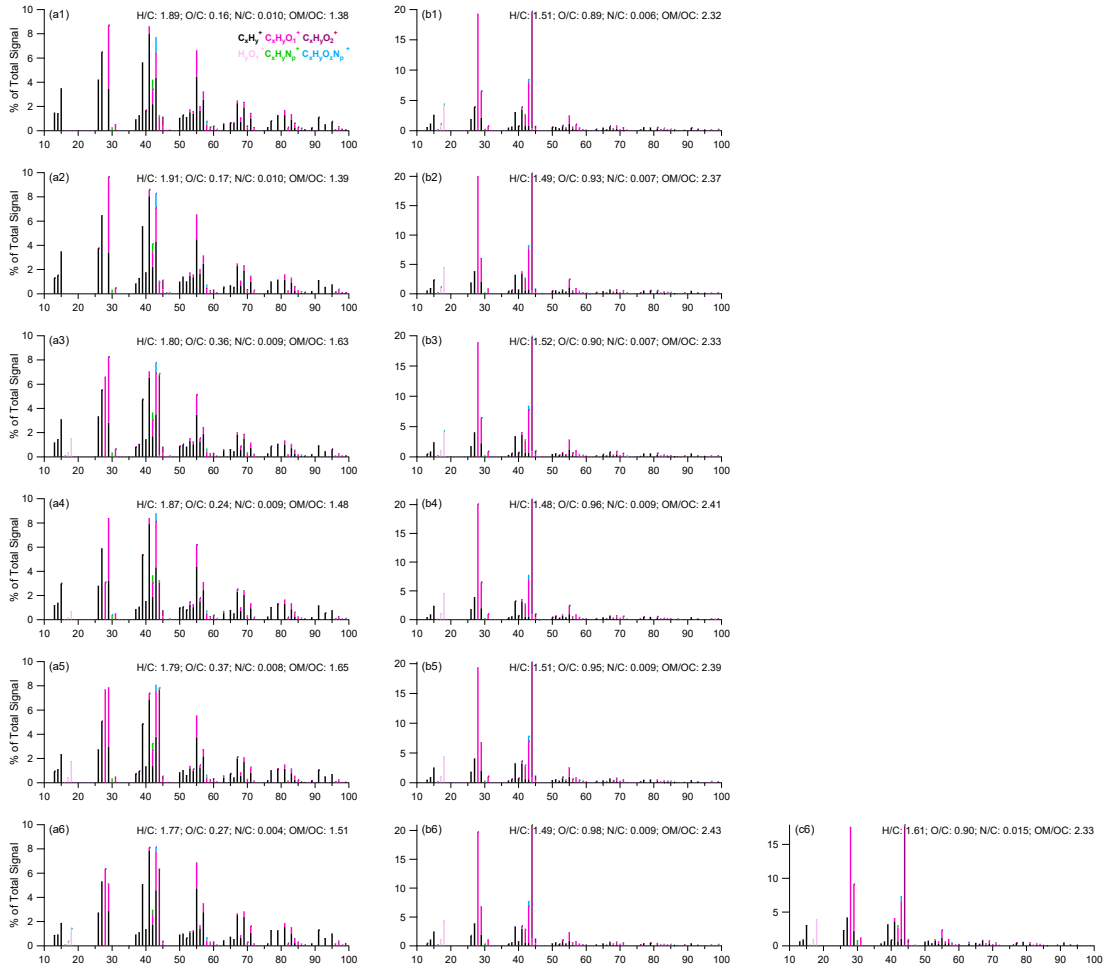


Figure S5. Size distributions of the total OA species (OOA1, OOA2, SOA, OPOA, POA, FFOA, BBOA) compared to the size distributions of total OA in (a) summer and (b) winter in Beijing, and (c) winter in Gucheng.



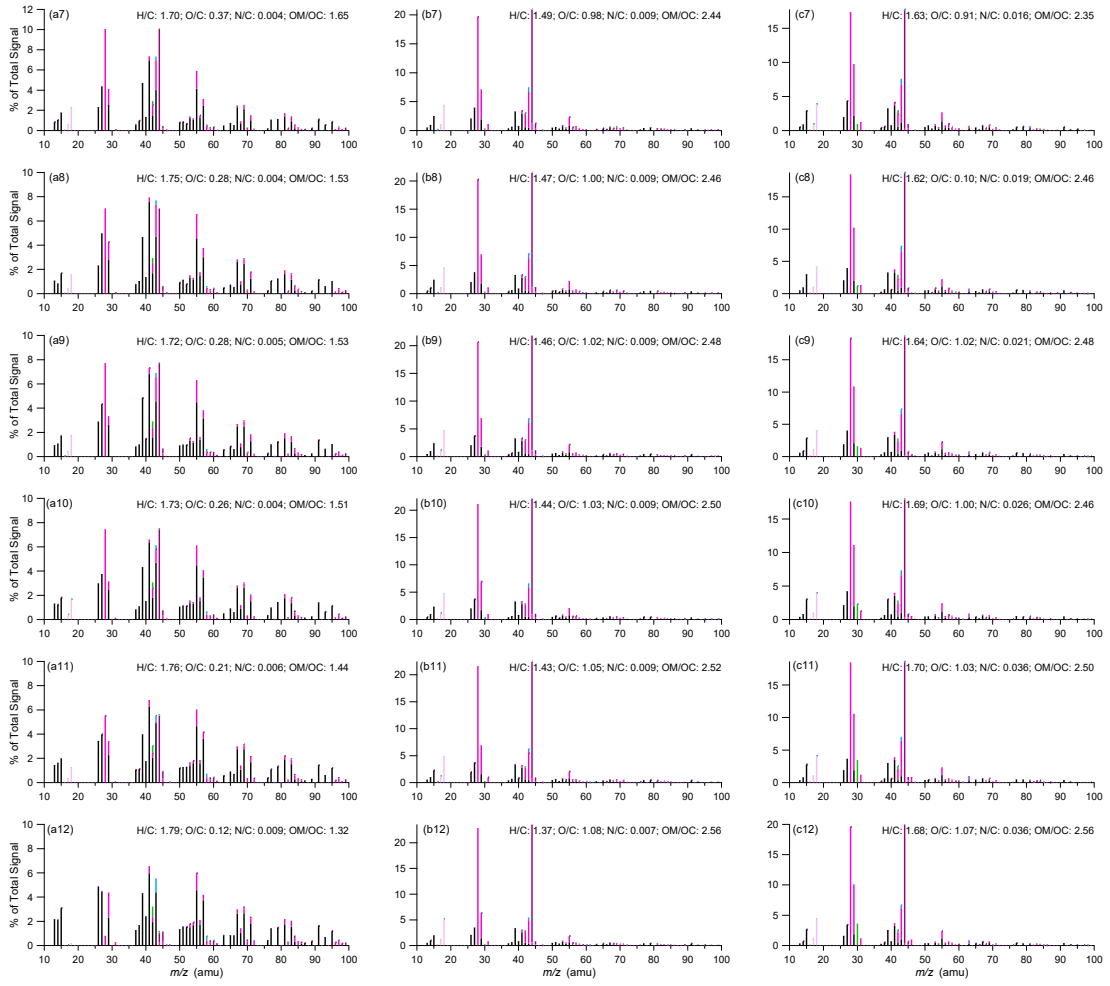
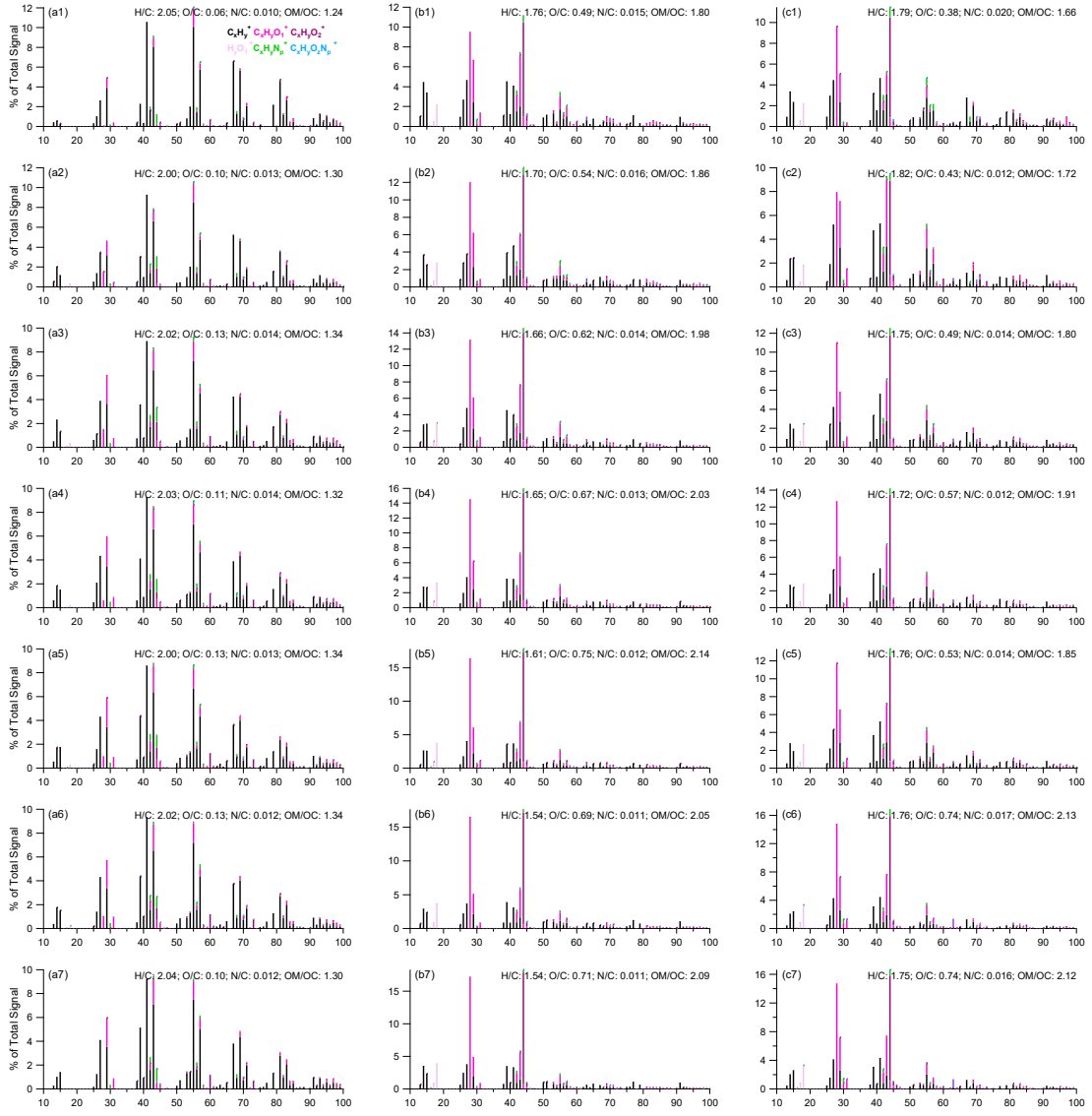


Figure S6. High-resolution mass spectra of (a1-a12) POA, (b1-b12) OOA1 and (c6-c12) OOA2 in Beijing in summer. The number of captions represents the sequence of the bin. A summary of size ranges of 14 bins in the range of 100 – 1000 nm is shown in Table. S1.



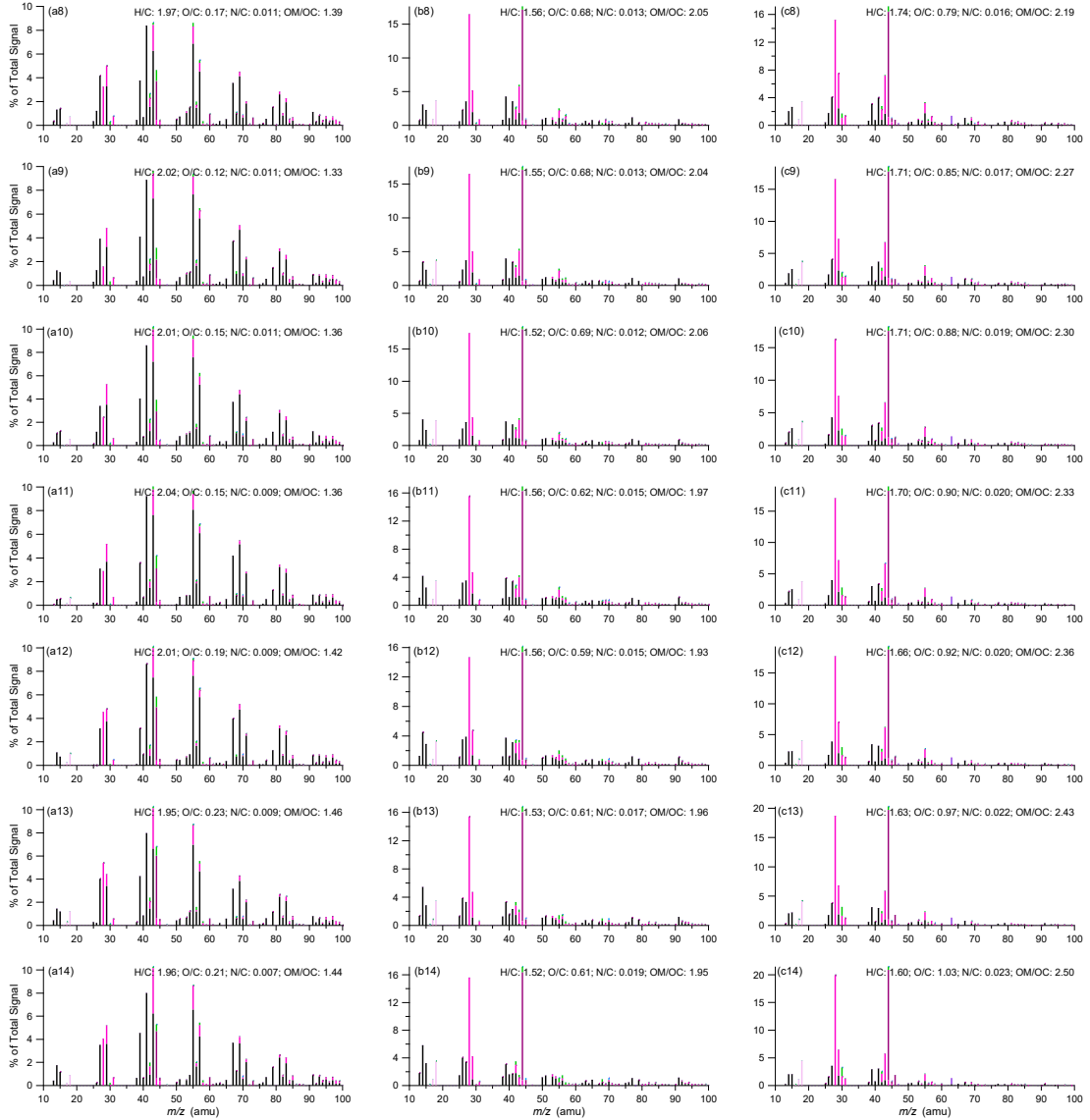
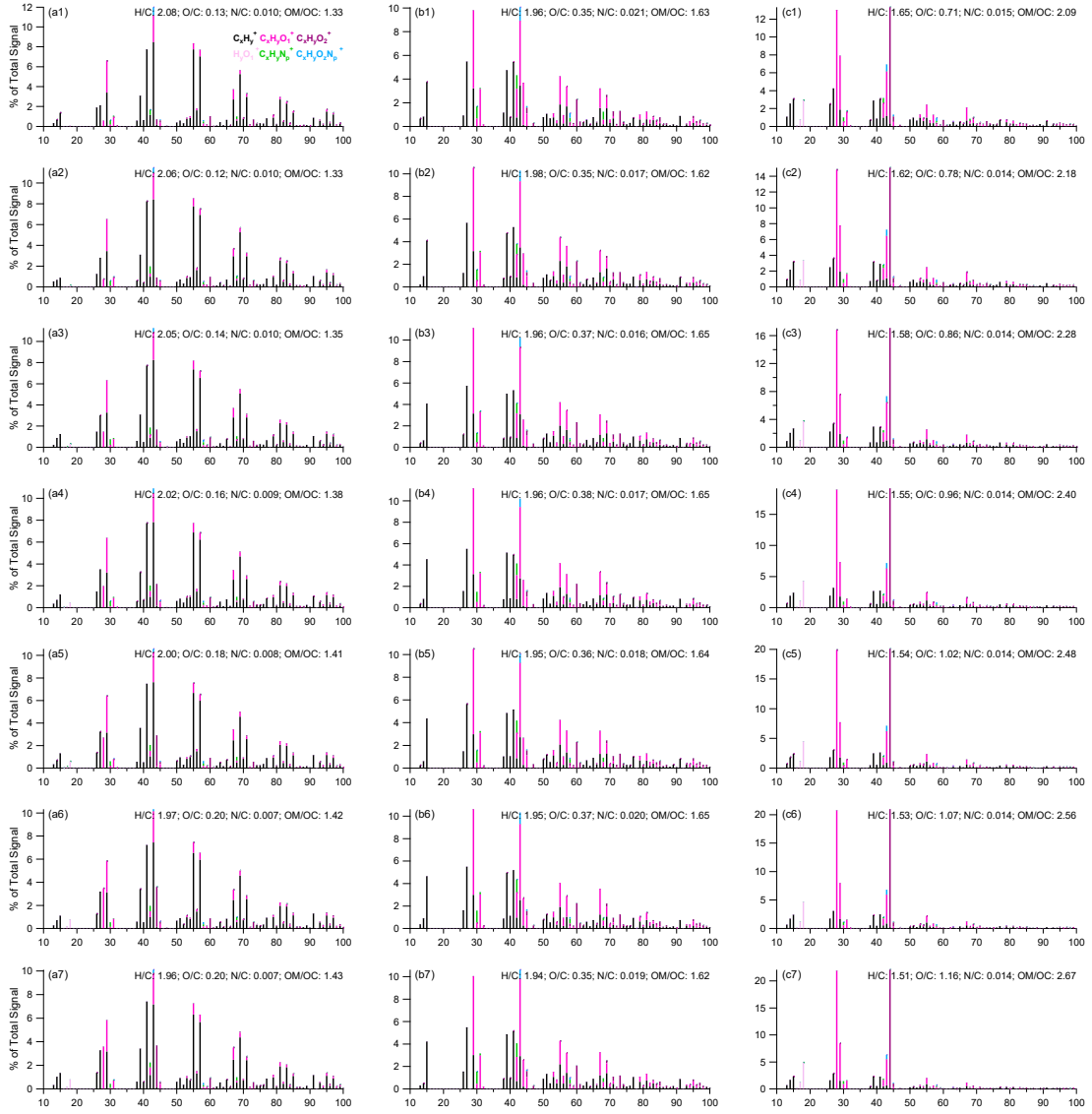


Figure S7. High-resolution mass spectra of (a1-a14) POA, (b1-b14) SOA and (c1-c14) OPOA in Beijing in winter. The number of captions represents the sequence of the bin. A summary of size ranges of 14 bins in the range of 100 – 1000 nm is shown in Table. S1.



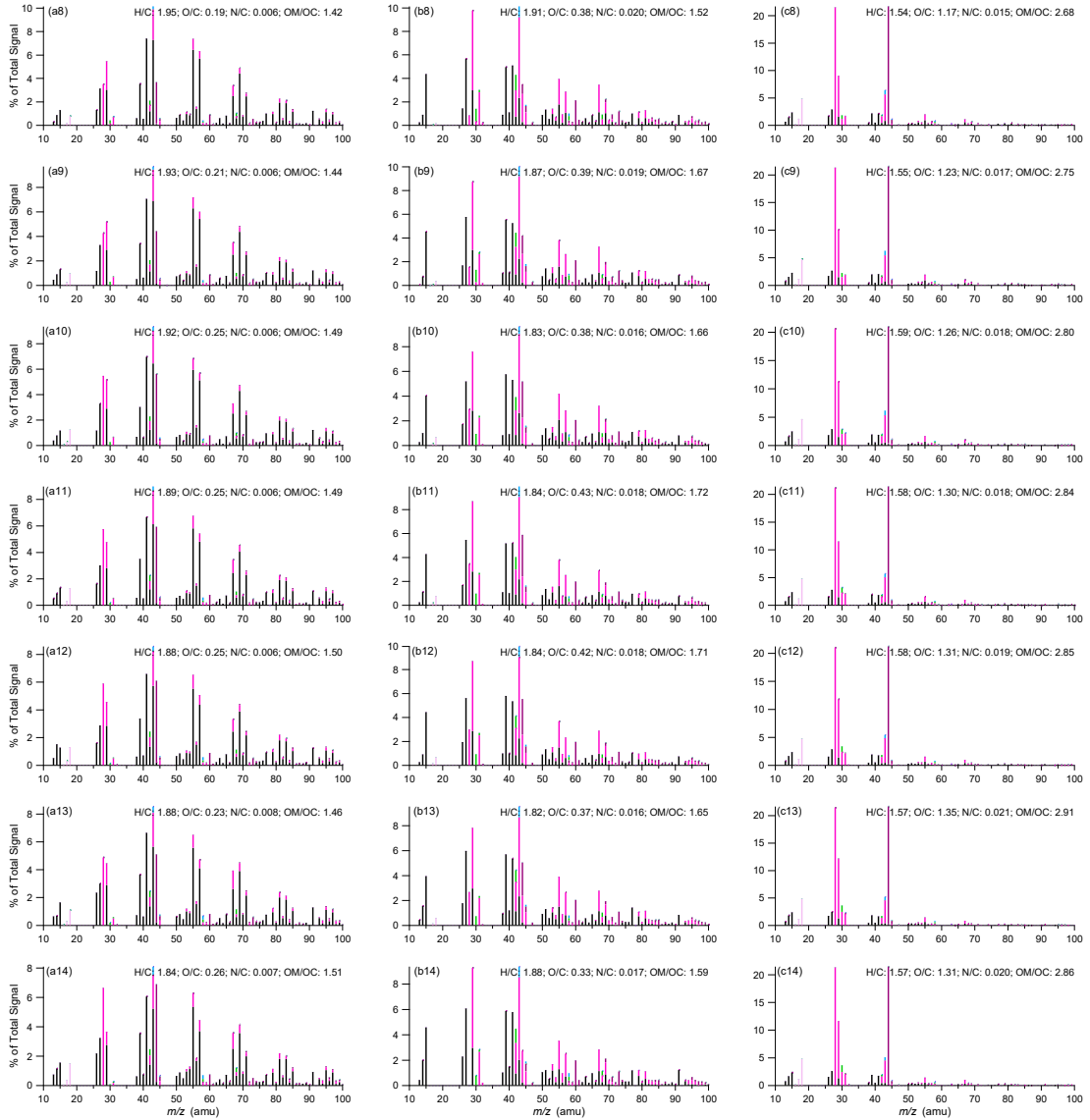


Figure S8. High-resolution mass spectra of (a1-a14) FFOA, (b1-b14) BBOA and (c1-c14) SOA in Gucheng in winter. The number of captions represents the sequence of the bin. A summary of size ranges of 14 bins in the range of 100 – 1000 nm is shown in Table. S1.

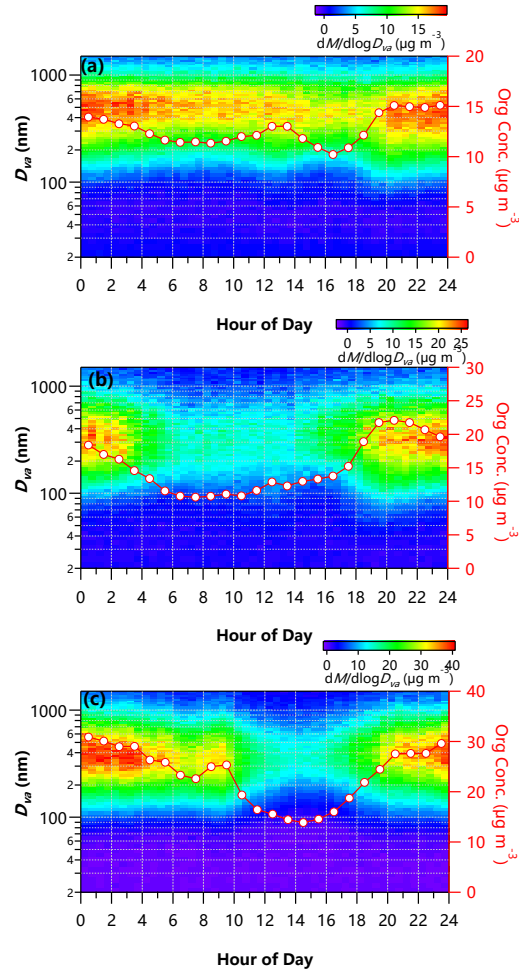


Figure S9. Diurnal evolution of the size distributions of OA in (a) summer and (b) winter in Beijing, and (c) winter in Gucheng.

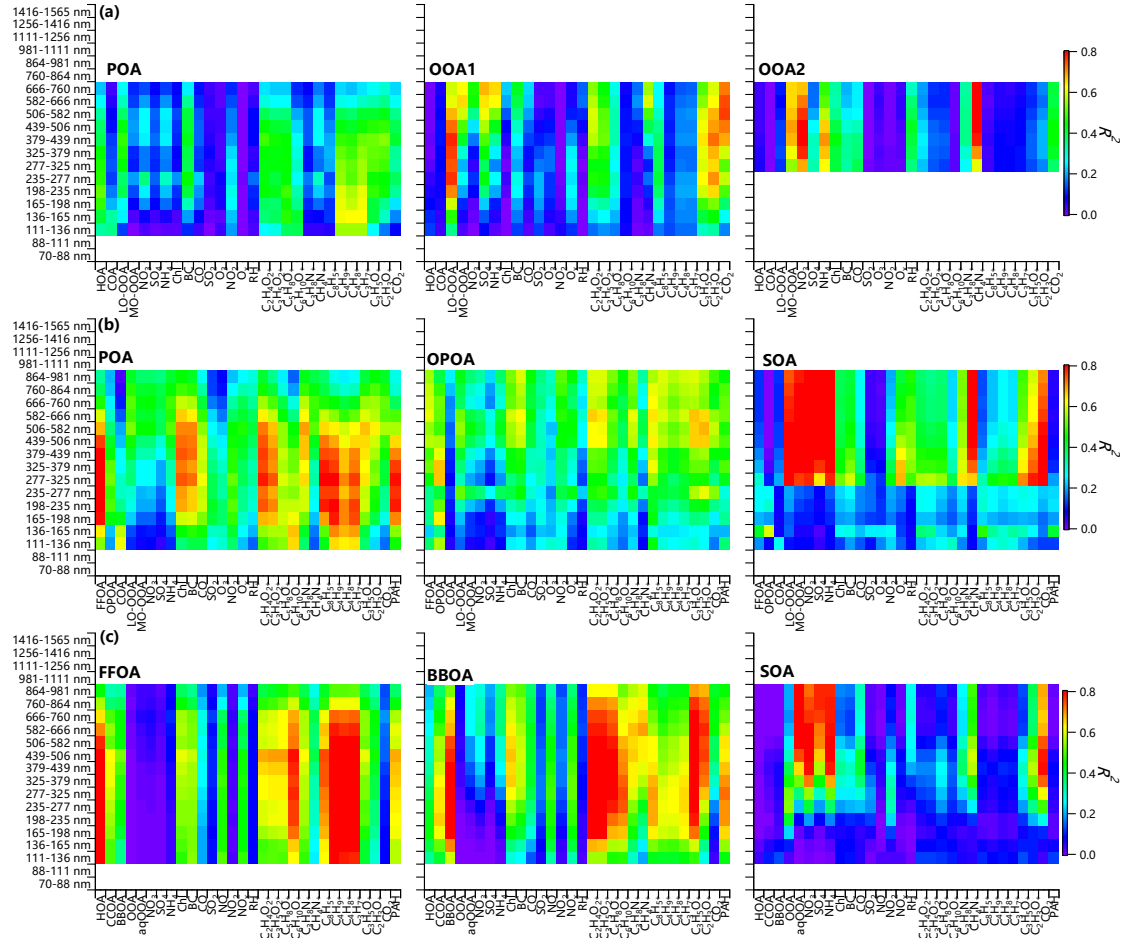


Figure S10. Correlations of OA factors and tracers in (a) summer and (b) winter in Beijing, and (c) winter in Gucheng in different size. POA (left), OOA1(middle) and OOA2(right) were identified in summer in Beijing. Comparatively, POA (left), OPOA (middle) and SOA (right) in Beijing and FFOA (left), BBOA (middle) and OOA(right) in Gucheng were identified during wintertime.

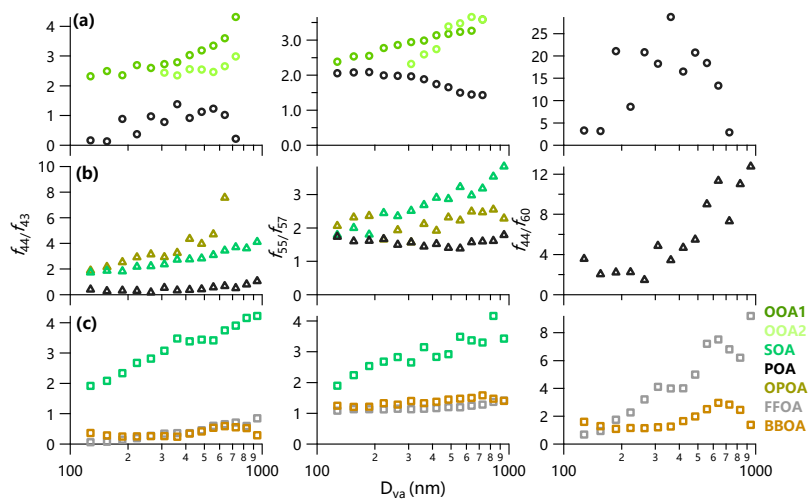


Figure S11. Size distributions of f_{44}/f_{43} (left), f_{55}/f_{57} (middle) and f_{44}/f_{60} (right) for OA factors in (a) summer and (b) winter in Beijing, and (c) winter in Gucheng.

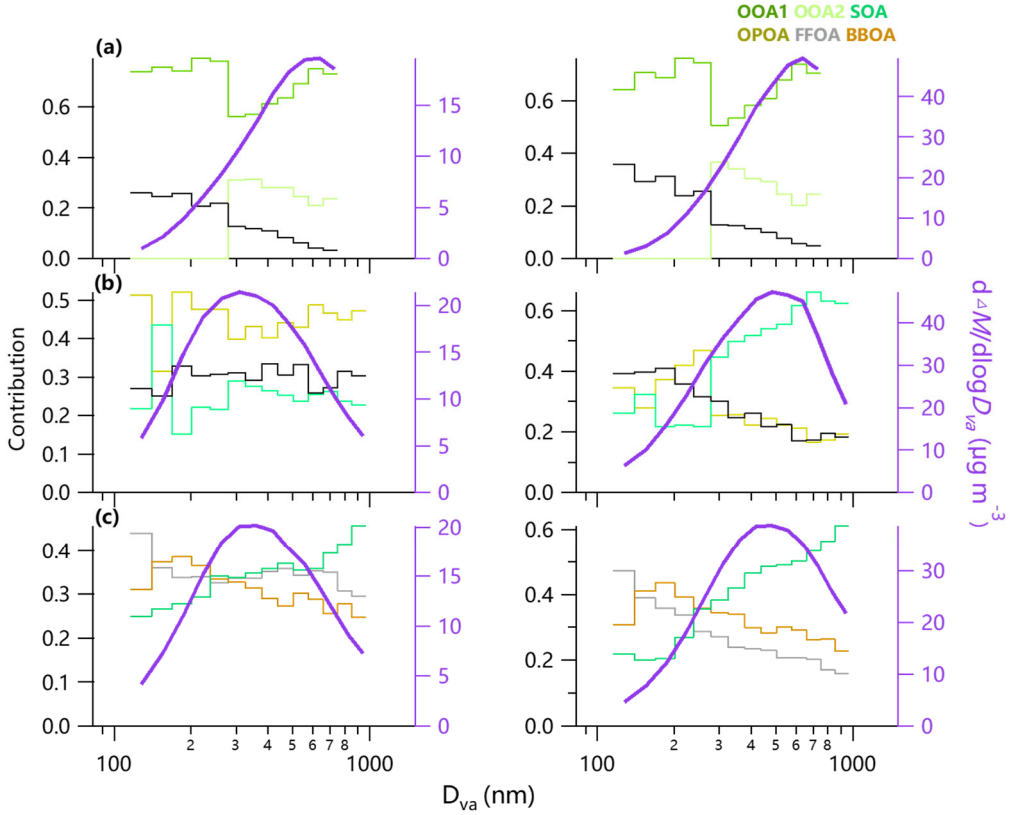


Figure S12. Contribution of increase in the concentrations of OA species during moderately (left, $35 \mu\text{g m}^{-3} < \text{NR-PM}_1 < 70 \mu\text{g m}^{-3}$) and seriously pollution (right, $\text{NR-PM}_1 > 70 \mu\text{g m}^{-3}$) in each size bin compared to clean days ($\text{NR-PM}_1 < 35 \mu\text{g m}^{-3}$) in (a) summer and (b) winter in Beijing, and (c) winter in Gucheng. The differences in OA loading between moderately pollution and clean days (left), seriously pollution and clean days (right) are also shown.

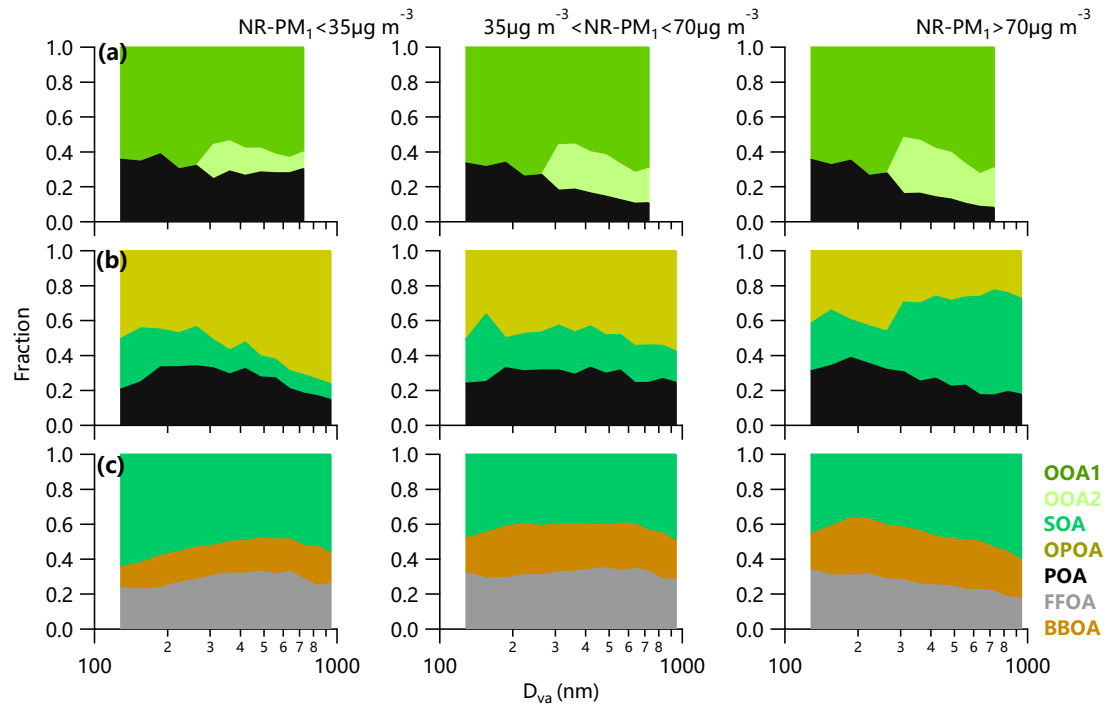


Figure S13. The contribution for OA factors at NR-PM₁ < 35 $\mu\text{g m}^{-3}$ (left), 35 $\mu\text{g m}^{-3}$ < NR-PM₁ < 70 $\mu\text{g m}^{-3}$ (middle) and NR-PM₁ > 70 $\mu\text{g m}^{-3}$ (right) in (a) summer and (b) winter in Beijing, and (c) winter in Gucheng.

Table S1. A summary of size ranges of 14 bins in the range of 100 – 1000 nm

| Bin number | PToF Size (nm) |
|------------|----------------|
| Bin#1 | 110.6-135.9 |
| Bin#2 | 135.9-164.8 |
| Bin#3 | 164.8-197.7 |
| Bin#4 | 197.7-235.1 |
| Bin#5 | 235.1-277.4 |
| Bin#6 | 277.4-325.1 |
| Bin#7 | 325.1-378.8 |
| Bin#8 | 378.8-438.9 |
| Bin#9 | 438.9-506.3 |
| Bin#10 | 506.3-581.7 |
| Bin#11 | 581.7-665.8 |
| Bin#12 | 665.8-759.7 |
| Bin#13 | 759.7-864.4 |
| Bin#14 | 864.4-981.0 |

Table S2. A summary of frequencies of three different PM levels

| | NR-PM ₁ < 35 µg m ⁻³ | 35 µg m ⁻³ < NR-PM ₁ < 70 µg m ⁻³ | NR-PM ₁ > 70 µg m ⁻³ |
|---------------|--|--|--|
| SummerBeijing | 57.3% | 30.9% | 11.8% |
| WinterBeijing | 58.1% | 27.6% | 14.3% |
| WinterGucheng | 25.2% | 37.2% | 37.6% |